Proceedings of the ASME 2010 29th International Conference on Ocean, Offshore and Arctic Engineering
OMAE 2010
June 6-11, 2010, Shanghai, China

OMAE2010-20077

COUPLING EFFECTS BETWEEN TANK SLOSHING AND MOTIONS OF A LNG CARRIER

Günther F. Clauss
Naval Architecture & Ocean Eng.
Technical University of Berlin
Germany
Email: clauss@naoe.tu-berlin.de

Daniel Testa*
Naval Architecture & Ocean Eng.
Technical University of Berlin
Germany
Email: testa@naoe.tu-berlin.de

Florian Sprenger*
Naval Architecture & Ocean Eng.
Technical University of Berlin
Germany
Email: f.sprenger@naoe.tu-berlin.de

ABSTRACT

Free liquid surfaces inside the cargo tanks of seagoing ships not only reduce the initial stability but also influence the seakeeping characteristics, in particular roll motions. Due to the increasing demand of liquefied natural gas (LNG), the concept of offshore processing or receiving terminals will gain in importance. Since pipelines are not economic for long distances, LNG is transported by shuttle carriers from remote marine locations for onshore energy supply. The loading/unloading procedure of an average carrier vessel takes 18 to 24 hours — a time span where the tanks are partially filled and feature free liquid surfaces. Depending on the filling level, the wave incident angle as well as the phase shift of tank sloshing and body motions, the characteristics of the vessel's response amplitude operators (RAO), especially the roll motion, are altering. This is ascribed to coupling effects between the moving liquid and the hull motions. Hence, the seakeeping characteristics have to be reappraised for each case. A 138,000 m^3 LNG carrier with four membrane tanks is numerically analysed with a potential theory based software at different filling levels and wave incident angles in frequency domain. For experimental validation, the tanks are filled with water. Optical motion sensors and transient wave packages are used to determine the RAOs in six degrees of freedom. Additionally, the forces and moments induced by the sloshing liquid are measured by six-component force sensors. On this basis, further computations with LNG are conducted. The focus of the investigations lies on the influence of sloshing on the surge and roll motions of the exemplarily chosen LNG carrier. Instead of one single resonance peak as for the solid filling case, the roll RAO of the dual-mass system features two peaks, whose magnitude and position depends on the filling level of the cargo tanks. But coupling effects due to resonant sloshing also affect longitudinal body motions. The knowledge of the altered seakeeping characteristics of LNG carriers due to free liquid surfaces is essential for save offshore transfer operations.

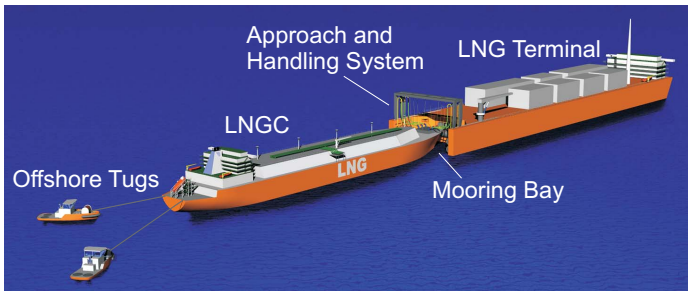

FIGURE 1. MPLS20 OFFSHORE LNG TRANSFER SYSTEM IN TANDEM CONFIGURATION

*Address all correspondence to these authors.

INTRODUCTION

For several decades, natural gas was merely a byproduct of oil production. Today, its importance as energy source is still growing. Large quantities of natural gas are produced from offshore fields, with associated problems of transportation to further onshore processing. Especially for remote marine gas fields, the deployment of LNG tank ships (Liquefied Natural Gas) is a more economic alternative to pipelines — with increasing significance (see RINA [1]).

As published by Cook [2], only one floating offshore LNG transfer system — based on the emergency unloading technology — was tested in calm water conditions and side-by-side configuration using 8" non-insulated composite hoses until today. However, Frohne et al. [3] state that the increasing loading capacity of currently built LNG carriers (up to 260,000 m^3) creates a new market for fast and safe loading/offloading concepts — i.e. larger pipe diameters and transfer operations in rough seas.

Offshore terminal designs for production and processing of natural gas are typically fixed at a certain location by turret mooring and transfer the liquefied gas to periodically operating shuttle tankers in side-by-side configuration.

In the framework of the joint research project *Maritime Pipe Loading System 20"* (MPLS20), an innovative offshore transfer system between a turret moored terminal barge and a shuttle carrier in tandem configuration is developed and analysed by Clauss et al. [4] and Hoog et al. [5]. *Brugg Pipe Systems* is designing a corrugated transfer pipe of 16" inner diameter for LNG loading/offloading — which is significantly exceeding currently existing pipe diameters and hence transfer rates. The work of *Nexans* focusses on the manufacturing technology of the vacuum insulated transfer pipes, *IMPaC Offshore Engineering GmbH* is in authority of the approaching and handling system and *Technical University Berlin* is conducting model tests as well as numerical simulations in order to analyse the hydrodynamical characteristics of the coupled system.

As fluid sloshing inside the cargo tanks significantly influences the vessel's seakeeping behavior, the knowledge of the expected filling height-dependent system motions during loading/offloading procedures is essential in order to assure safe operations. This scenario is numerically and experimentally analysed for the exemplary LNG carrier described by Tab. 1 and Tab. 2, respectively.

Newman [6] conducted numerical investigations where coupled vessel motions of a spheroidal hull with three partially filled tanks were analysed using a linear potential theory based approach. Gaillarde et al. [7] carried out model tests as well as numerical simulations for a LNG-FPSO, assessing coupled roll motions at different filling ratios. Molin et al. [8, 9] proposed a theoretical method to predict the combined dynamics of a barge hull and sloshing in internal tanks and also conducted experimental studies focussing on high tank filling levels and roof impacts for different tank geometries. Lee et al. [10] analysed the effects of tank sloshing on roll and pitch motions of an LNG vessel.

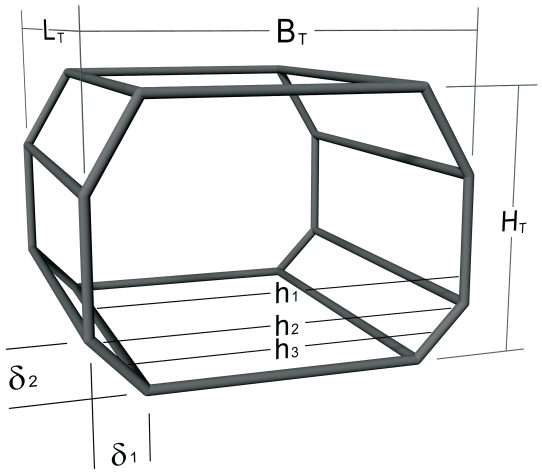

FIGURE 2. PRINCIPAL 3D-SKETCH OF THE PRISMATIC TANK WITH ALL RELEVANT DIMENSIONS

In this paper the motion behavior of a LNG-Carrier (LNGC) with 138,000 m^3 loading capacity and 4 membrane tanks is systematically analysed for four different filling levels (100 % (solid filling), h_1 = 30 %, h_2 = 20 % and h_3 = 10 % filling height) at a constant draught of 12 m and 100 m water depth. Tab. 1 shows the main dimensions of the LNGC and the cargo tanks. For clarification, Fig. 2 provides a 3D sketch of the prismatic tank. As

TABLE 1. MAIN DIMENSIONS OF THE LNGC AND THE TANKS (FULL SCALE)

Parameter	Dimension
Length over all	282 m
Breadth	42 m
Draught	12 m
Height	26 m
Displacement	103,921 m^3
Loading capacity	138,000 m^3
Tank length L_T	38.3 m
Tank breadth B_T	35.8 m
Tank height H_T	26.1 m
δ_1	4.65 m
δ_2	5.0 m

it is not feasible to carry out model tests with hazardous liquids like LNG, a numerical model is firstly validated and calibrated for water filling by comparing Response Amplitude Operators (RAO). Subsequently, numerical simulations with LNG filling are conducted.

EXPERIMENTAL SETUP

For experimental investigations, a glass-fibre reinforced plastic (GRP) model of the LNG carrier as shown in Fig. 3, top, and described in Tab. 1 is built at a scale of 1:100. All tests are carried out in the seakeeping basin of Technical University Berlin. The carrier model is soft-moored and equipped with four wireless, individually pulsed infrared sensors. The body motions in six degrees of freedom are precisely tracked by five cameras mounted on a carriage above the basin with a tracking range of 8×10 m. Also, the foremost and sternmost tanks are placed on six-component force sensors to measure the forces and moments between tanks and hull (see Fig. 3, centre). A ship-fixed camera located at the stern of the vessel records the interior fluid motions in the tanks. Test series with filling levels of 10 %, 20 % and 30 % water in all four tanks have been conducted at a constant draught of 12 m (full scale). In order to analyse the seakeeping characteristics of the carrier in these different loading conditions in frequency domain, transient wave packet technique as proposed by Clauss and Kühnlein [11] is applied.

In Tab. 2, all relevant model test parameters are listed in dependency of the filling ratio. The filling height (f.h.) is denoted by h, the mass of water inside the four tanks by m_T, the height of the centre of gravity above keel for the hull including ballast by KG_H and the radii of gyration by i_{xx}, i_{yy} and i_{zz}, respectively.

TABLE 2. MODEL TEST PARAMETERS IN DEPENDENCY OF THE FILLING HEIGHT (FULL SCALE)

Parameter	10 % f.h.	20 % f.h.	30 % f.h.	solid filling
h [m]	2.6	4.9	7.9	—
m_T [kg]	1.05e^{07}	2.16e^{07}	3.97e^{07}	—
KG_H [m]	12.85	12.36	12.57	15.13
$i_{xx,H}$ [m]	14.62	14.67	15.22	12.57
$i_{yy,H}$ [m]	80.63	82.61	82.14	72.17
$i_{zz,H}$ [m]	81.18	83.25	82.48	72.95

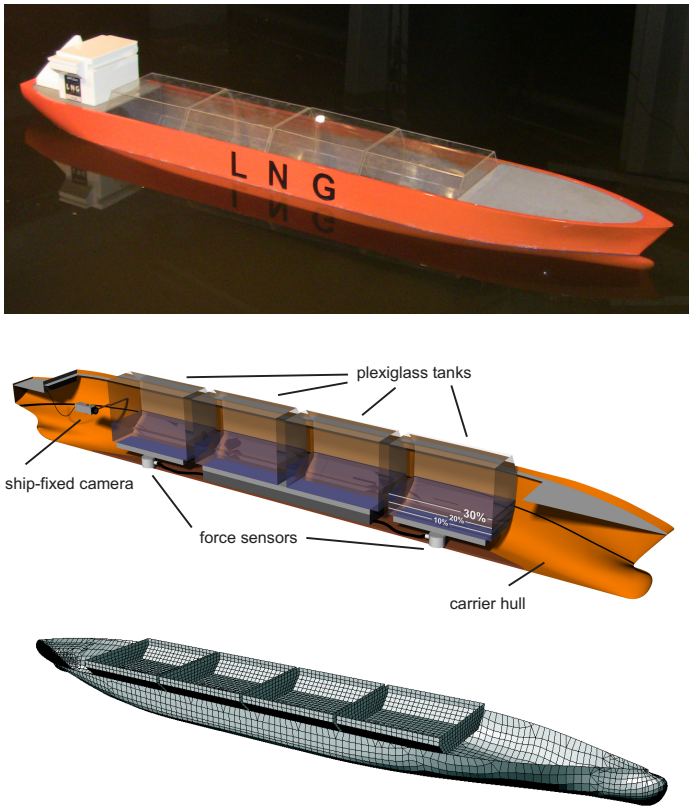

FIGURE 3. GRP MODEL OF THE LNG CARRIER IN THE SEAKEEPING BASIN AT A MODEL SCALE OF 1:100 (TOP); LONGITUDINAL CUT THROUGH A 3D SKETCH OF THE LNGC SHOWING THE FOUR INTEGRATED PLEXIGLASS TANKS, THE TWO SIX-COMPONENT FORCE SENSORS AND THE ON-BOARD CAMERA (CENTRE); LNGC DISCRETISATION WITH 6432 PANELS FOR NUMERICAL ANALYSES WITH 30 % TANK FILLING (BOTTOM)

NUMERICAL SETUP

All numerical simulations are conducted in frequency domain with the radiation-diffraction panel code WAMIT (Wave Analysis at Massachusetts Institute of Technology, [12]), which is based on potential theory and is widely accepted as a reliable tool for hydrodynamic analyses in offshore technology. From version 6.2 on, WAMIT is capable of analyzing internal tanks and linear tank/ship interaction. As described by Newman [6], the interior wetted tank surfaces are considered as an extension of the exterior wetted body surface to form one global boundary surface with two independent fluid domains and separate sets of linear equations. Tank filling heights as well as the density of the internal fluid can be chosen arbitrarily (in this case: water 998.2 kg/m^3, LNG 435 kg/m^3).

Since only potential damping is considered in this linear ap-

proach, viscous damping effects — in particular for roll motions — have to be taken into account by modifying the respective damping terms for the equations of motion. The viscous part of the total damping is determined by subtracting the potential damping calculated by WAMIT from the total damping determined by decay tests with the carrier hull at solid filling condition. Since the model tests do not take into account scaled viscosities (exclusively Froude-compliant), the total damping is overestimated compared to full scale values. Based on these results, an external viscous damping matrix is implemented in the numerical code. Fig. 3, bottom, shows the discretisation of the carrier hull and the four prismatic tanks by 6432 panels for the 30 % tank filling case.

SLOSHING VALIDATION WITH WATER

Since hazardous liquids like LNG cannot easily be used in model tests, this cargo can only be investigated numerically. In order to calibrate and validate the numerical code, model test and calculations with water are conducted first. Three different filling heights h are considered, but in the following, 30 % tank filling is regarded exclusively, i.e. $h = 7.9$ m (full scale). The validation of the numerical method is achieved by comparison of RAOs of the rigid body motions of the LNGC with partially filled tanks. In Fig. 4, the numerically computed RAOs for surge and pitch (incident wave angle $\beta = 180°$, blue box) as well as sway and roll ($\beta = 90°$, orange box) are compared to model test results.

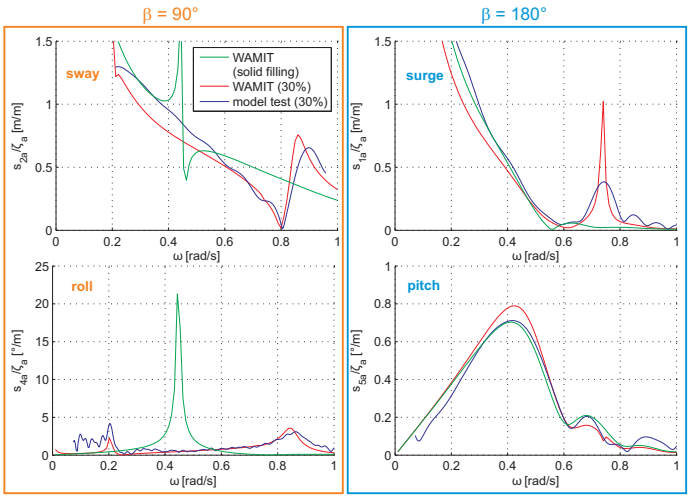

FIGURE 4. COMPARISON BETWEEN WAMIT COMPUTATIONS (SOLID FILLING AND 30 % FILLING HEIGHT) AND MODEL TEST RESULTS FOR SURGE AND PITCH ($\beta = 180°$, BLUE BOX) AS WELL AS SWAY AND ROLL ($\beta = 90°$, ORANGE BOX) MOTIONS AT 30 % TANK FILLING (WATER)

Model test results and numerical computations show excellent agreement. For highlighting the deviating characteristics between solid filling and partial filling, Fig. 4 also includes the case without free fluid surfaces computed by WAMIT. For solid filling, the surge motion continuously converges to zero in short waves while for 30 % filling height, a prominent peak appears at $\omega = 0.74$ rad/s. The pitch motion for the partial filling case shows no significant deviations compared to solid filling. In beam seas ($\beta = 90°$), the sway motion with free fluid surfaces features a local maximum at $\omega = 0.86$ rad/s instead of $\omega = 0.44$ rad/s, which can be ascribed to coupling with the roll motion, that shows the most significant deviations. Instead of one high solitary resonance peak as for solid filling at $\omega = 0.44$ rad/s, the roll RAO for 30 % filling height features two smaller peaks — one at a lower ($\omega = 0.2$ rad/s) and one at a higher wave frequency ($\omega = 0.86$ rad/s). The internal fluid acts as a roll damping system leading to peaks of low magnitude outside the region where significant spectral wave energy is usually expected. The phenomenon of the drastically changing roll characteristics can be ascribed to the dual-mass system of carrier and freely moving interior fluid. In order to interpret the roll motion characteristics with free fluid surfaces inside the cargo tanks, Fig. 5 shows snap shots of the fluid motion inside the sternmost tank taken from the on-board camera for 30 % filling height. The three pictures in the top row show fluid motion in regular waves ($\beta = 90°$) with $\omega = 0.2$ rad/s, i.e. the low-frequency roll peak, the centre pictures show snapshots of the fluid motion for the high-frequency roll peak ($\omega = 0.86$ rad/s) and the bottom row represents the surge motion peak at $\omega = 0.74$ rad/s.

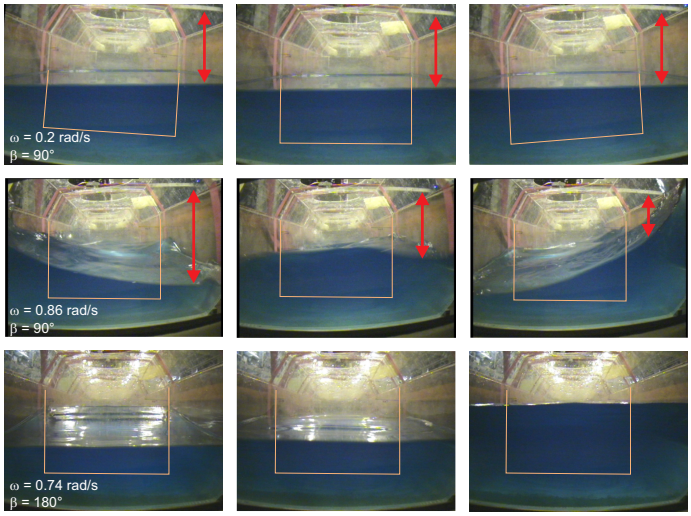

FIGURE 5. SNAP SHOTS FROM THE ON-BOARD CAMERA IN REGULAR WAVES. $\omega = 0.2$ rad/s (TOP, $\beta = 90°$), $\omega = 0.86$ rad/s (CENTRE, $\beta = 90°$) AND $\omega = 0.74$ rad/s (BOTTOM, $\beta = 180°$)

- For ω = 0.2 rad/s, large roll amplitudes and roll periods can be observed, but the water inside the tanks does not move, the free surface remains still — it appears the ship 'rolls around' its liquid cargo. Please note that although the camera is ship-fixed, the picture frames for this case have been rotated for the observer to remain in phase with the interior water. The red arrows indicate the vertical distance from the water level inside the tank to a rail in level with the basin still water level. It can be observed that this distance remains unchanged.
- For ω = 0.86 rad/s, large roll amplitudes and short roll periods of the vessel can be observed. Inside the tank, strong sloshing motions become evident. From the red arrows, it can be concluded that the vessel's roll motions and the fluid motions inside the tanks are in phase, i.e. the sloshing liquid enforces the roll motions and vice versa.
- For ω = 0.74 rad/s, increased surge motions of the LNG carrier can be observed and the water inside the tank shows moderate sloshing motions in longitudinal direction.

For the interpretation of the characteristics of the 30 % filling height RAOs in Fig. 4, the natural sloshing frequencies of the cargo tanks are determined. According to Faltinsen and Timokha [13] the natural transverse sloshing frequency of the i^{th} mode of a rectangular tank is given by the expression

$$\omega_{r,i} = \sqrt{g\frac{\pi i}{B_T}\ tanh(\frac{\pi i}{B_T}h)}. \qquad (1)$$

For prismatic tanks with chamfered bottom, Faltinsen and Timokha [13] also proposed a correction factor:

$$\frac{\omega_{r,i}'^2}{\omega_{r,i}^2} = 1 - \frac{\frac{\delta_1}{\delta_2}\ sinh^2(\frac{\pi i\delta_2}{B_T}) - \frac{\delta_1}{\delta_2}\ sin^2(\frac{\pi i\delta_1}{B_T})}{\pi i\ sinh(\frac{2\pi ih}{B_T})}, \qquad (2)$$

giving the percentaged deviation compared to rectangular tanks. $\omega'_{r,i}$ is the corrected natural frequency of the i^{th} mode.

TABLE 3. FIRST NATURAL TANK SLOSHING FREQUENCIES IN TRANSVERSAL DIRECTION

Filling Level	$\omega_{r,1}$ (transversal)
10%	0.52 rad/s
20%	0.60 rad/s
30%	0.72 rad/s

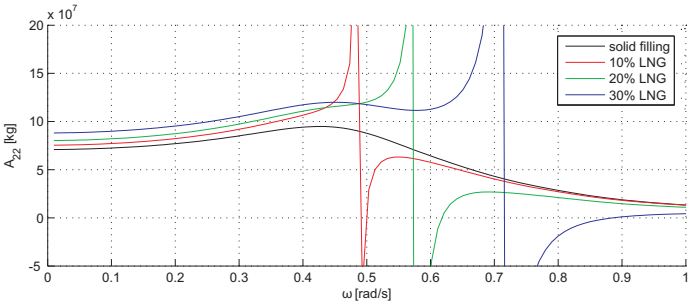

FIGURE 6. ADDED MASSES FOR SWAY AT DIFFERENT FILLING HEIGHTS (FULL SCALE); THE PEAKS REPRESENT THE NATURAL TANK SLOSHING FREQUENCIES IN TRANSVERSAL DIRECTION

In Tab. 3, the first transverse sloshing modes (i = 1) for the tanks shown in Fig. 2 are listed in dependency of the filling height.

By analysing the added masses calculated by WAMIT in transverse (A_{22}, sway) direction (see Fig. 6), these frequencies can be identified by discontinuities. (Please note that the results

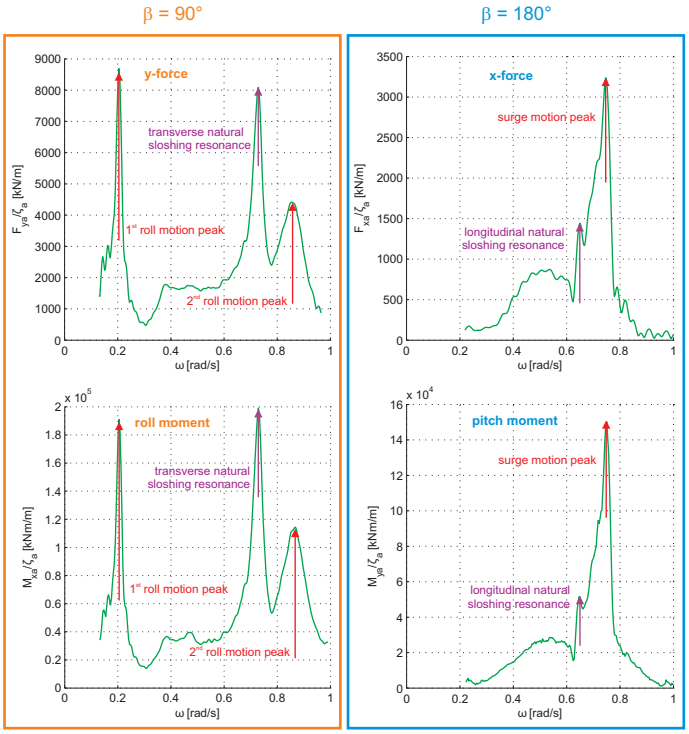

FIGURE 7. MEASURED Y-FORCE AND ROLL-MOMENT RAOS (β = 90°, LEFT, ORANGE BOX) AS WELL AS X-FORCE AND PITCH-MOMENT RAOS (β = 180°, RIGHT, BLUE BOX) WITH INDICATED CAUSES FOR PEAKS (FULL SCALE)

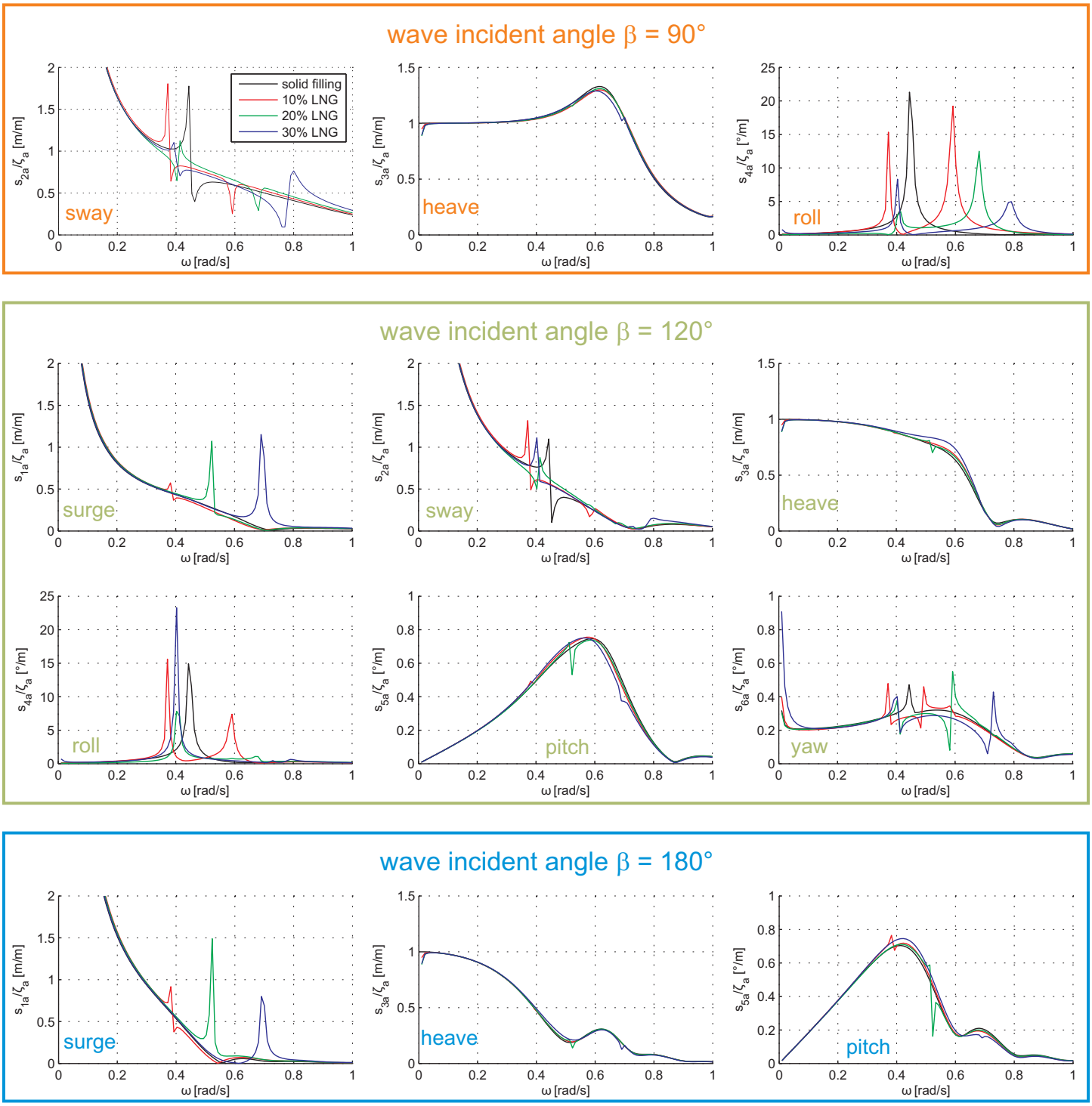

FIGURE 8. COMPARISON OF RAOS FOR DIFFERENT LNG FILLING LEVELS AND WAVE INCIDENT ANGLES OBTAINED BY WAMIT

become better for higher filling levels, since Eqs. (1) and (2) are valid only for filling levels above the chamfers.)

Considering the forces and moments induced by the sloshing fluid on the carrier hull, Fig. 7 shows that the first natural sloshing frequencies are reflected in these RAOs, resulting in strong peaks in the transversal direction ($\beta = 90°$, $\omega = 0.72$ rad/s, see orange box in Fig. 8) and small peaks in the longitudinal direction ($\beta = 180°$, $\omega = 0.68$ rad/s, see blue box in Fig. 8). As indicated, the other maximum values are caused by peaks in the respective vessel motion RAOs. However, Fig. 4 shows that the motion peaks related to sloshing phenomena do not exactly appear at the natural tank sloshing frequency but are shifted towards higher frequencies where the magnitude. This deviation depends on the fluid mass inside the tanks.

SLOSHING ANALYSES WITH LNG

In the preceding section, the numerical approach is successfully validated for water filling. Now, the cargo tanks are simulated with LNG instead, which cannot be achieved by model tests. In Fig. 8, the numerical results for 10 %, 20 % and 30 % LNG filling ratio are presented. Inside the orange box (top), sway, heave and roll for $\beta = 90°$ are presented. The heave motion shows no dependency on the filling ratio, while sway and in particular roll feature significant changes in the motion characteristics. Similar to the observations for water filling in the previous section, one low-frequency and one high-frequency peak appears. For higher filling ratios, the high-frequency peak shifts into higher frequencies while it decreases. Due to the different densities of water ($\rho = 998.2$ kg/m^3) and LNG ($\rho = 435$ kg/m^3), the roll maxima for both cases are not identical. As Fig. 9 illustrates for different filling levels, the high-frequency peaks (related to the transversal sloshing resonances) for LNG appear at lower frequencies compared to water while the low-frequency peaks (rigid body resonances) are depending on the hull and ballast mass distribution. The sloshing induced high-frequency roll peaks appear close to the transversal sloshing resonance modes, but the distance $\Delta\omega$ between the natural sloshing frequency and the actual peak in the roll RAO increases with increasing fluid mass — i.e. filling height and higher fluid densities.

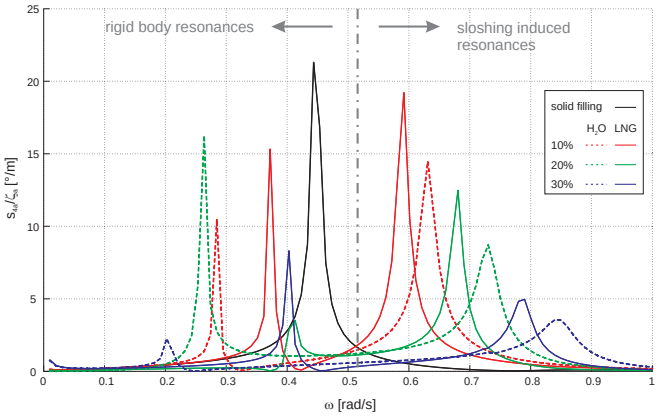

FIGURE 9. COMPARISON OF THE ROLL MOTION RAOS ($\beta = 90°$) FOR DIFFERENT FILLING LEVELS OF WATER AND LNG

For $\beta = 120°$, surge, sway, heave, roll, pitch and yaw RAOs are shown inside the green box (centre) and inside the blue box (bottom) surge, heave and pitch RAOs are presented for $\beta = 180°$. Again, it becomes apparent that free liquid surfaces do not influence heave and pitch motions, but surge and roll in particular. The surge peak also shifts to higher frequencies for increasing filling ratios, since it is caused by the resonant longitudinal sloshing.

CONCLUSIONS

Free liquid surfaces in internal cargo tanks significantly influence vessel motion characteristics. Especially roll ($\beta = 90°$ and 120°) and surge ($\beta = 180°$ and 120°) feature new maximum values (two roll peaks, one surge peak) which are changing in frequency and magnitude in dependency of the filling height. Heave and pitch motions on the other hand are not significantly changing.

By conducting model tests with different filling ratios of water (10 %, 20 % and 30 %), the numerical approach is successfully validated. Detailed analyses of the experimental and numerical results (including force and moment measurements) reveal interesting interactions. It is observed that the natural sloshing frequencies of the tanks strongly influence the force and moment RAOs, measured between tanks and carrier hull, which feature peaks caused by resonant tank sloshing as well as resonant body motions. In the longitudinal direction surge shows a prominent peak close to the first longitudinal natural sloshing frequency, and in transverse direction roll and sway RAOs feature peaks close to the first transverse natural sloshing frequency.

Calculations with LNG show the same tendencies as for water, but with different peak characteristic, caused by the lower density of the liquefied gas.

PERSPECTIVES

Based on these results, potential for further research work arises. In the previous investigations, only equally filled tanks are investigated. In case of different filling heights inside the interior tanks, the motion behavior of the carrier will be even more complicated. Also, the influence of different tank types as spherical tanks and bilobe tanks on the motion characteristics will be considered numerically.

Due to the minimum bending radius of the transfer pipes, the relative x- and z-motions between terminal and carrier ves-

sel of the MPLS20 system are restricted to $x_{rel} = \pm 2$ m and $z_{rel} = \pm 5$ m. On this basis, the operational range of the multi-body system in tandem configuration will be determined numerically in dependency of the filling height. Fig. 10 shows the tolerable sea states (JONSWAP spectra, 0.1 s $\leq T_0 \leq$ 15 s) related to the given relative motion limitations of the transfer pipe connecting points for an exemplary LNG filling height of 20 % and wave incident angles ($\beta = 90°$, $\beta = 120°$ and $\beta = 180°$). It can be

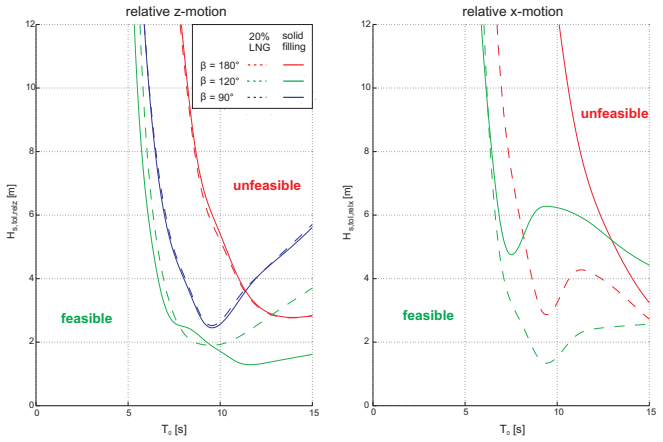

FIGURE 10. TOLERABLE SEA STATES FOR DIFFERENT LNG FILLING HEIGHTS AND WAVE INCIDENT ANGLES RELATED TO THE LIMITS OF THE RELATIVE Z- (LEFT) AND X-MOTIONS (RIGHT) OF THE TRANSFER PIPE CONNECTION POINTS

observed that the operational range due to the relative z-motion restriction is not influenced by sloshing motions with 20 % LNG filling height in the tanks (except for $\beta = 120°$, where slight deviations occur), while the relative x-motion limitation shows significant influences leading to a decreased operational range for 20 % LNG filling height and all wave incident angles. On basis of this data, stochastic downtime analyses will be conducted for locations in the North Sea region.

ACKNOWLEDGMENT

The authors wish to express their gratitude to the German Federal Ministry of Economics and Technology (BMWi) and Project Management Jülich (PTJ) for funding the joint research project '*MPLS20 — Maritime Pipe Loading System 20*"' (FKZ 03SX240D), in particular to Dipl.-Ing. Barbara Grothkopp and Dipl.-Betriebswirtin Cornelia Bude for their excellent support. Furthermore, we want to thank our project partners '*IMPaC Engineering*','*Brugg Pipe Systems*' and '*Nexans*' for their support. Many thanks also to our colleague at Technical University Berlin, Dipl.-Ing. Matthias Dudek for his contribution to this paper and to cand. ing. Basil Bodemann for his support during the model tests.

REFERENCES

[1] The Royal Institute of Naval Architects, 2006. "Gas ships: Trends and Technology".

[2] Cook, J. W., 2006. "Gulf Gateway Energy Bridge - The First Year of Operations and the Commercial and Operational Advantages of the Energy Bridge Technology". In Proceedings of the Offshore Technology Conference. OTC 18396.

[3] Frohne, C., Harten, F., Schippl, K., Steen, K. E., Haakonsen, R., Eide, J., and Høvik, J., 2008. "Innovative Pipe System for Offshore LNG Transfer". In Proceedings of the Offshore Technology Conference. OTC 19239.

[4] Clauss, G., Sprenger, F., Testa, D., Hoog, S., and Huhn, R., 2009. "Motion Behaviour of a New Offshore LNG Transfer System at Harsh Operational Conditions". In Proceedings of the 28 th Conference on Offshore Mechanics and Arctic Engineering.

[5] Hoog, S., Koch, H., Huhn, R., Frohne, C., Homann, J., Clauss, G., Sprenger, F., and Testa, D., 2009. "LNG Transfer in Harsh Environments — Introduction of a New Concept". In Proceeding of the Offshore Technology Conference. OTC 19866.

[6] Newman, J. N., 2005. "Wave effects on vessels whith internal tanks". In Proceedings of the 20 th International Workshop on Water Waves and Floating Bodies. Longyearbyen, Svalbard.

[7] Gaillarde, G., Ledoux, A., and Lynch, M., 2004. "Coupling Between Liquefied Gas and Vessel's Motion for Partially Filled Tanks: Effect on Seakeeping". In Proceedings of Design & Operation of Gas Carriers.

[8] Molin, B., Remy, F., Rigaud, S., and de Jouette, C., 2002. "LNG-FPSO's: frequency domain, coupled analysis of support and liquid cargo motions". In Proccedings of the 10 th Congress of the International Maritime Association of the Mediterranean.

[9] Molin, B., Remy, F., Ledoux, A., and Ruiz, N., 2008. "Effect of Roof Impacts on Coupling Between Wave Response and Sloshing in Tanks of LNG-Carriers". In Proceedings of the 27 th International Conference on Offshore Mechanics and Arctic Engineering.

[10] Lee, S., Kim, M., Lee, D., and Shin, Y., 2007. "The Effects of Tank Sloshing on LNG Vessel Repsonses". In Proceedings of the 26 th International Conference on Offshore Mechanics and Arctic Engineering.

[11] Clauss, G. F., and Kühnlein, W. L., 1997. "A new tool for seakeeping tests – nonlinear transient wave packets". In Proceedings of the 8 th Int. Conference on the Behaviour of Offshore Structures (BOSS), pp. 269–285.

[12] Massachusetts Institute of Technology, 2006. *WAMIT Version 6.4*. Userguide.

[13] Faltinsen, O., and Timokha, A., 2009. *Sloshing*. 1 st edition. Cambridge University Press.